Journal of Applied Polymer Science

Thermal Decomposition of Energetic Thermoplastic Elastomers of Poly(glycidyl nitrate)

Zaijuan Zhang, Gang Wang, Nan Luo, Muhua Huang, Miaomiao Jin, Yunjun Luo
School of Materials Science and Engineering, Beijing Institute of Technology, Beijing 100081, People's Republic of China
Correspondence to: Y. Luo (E-mail: yjluo@bit.edu.cn)

ABSTRACT: Energetic thermoplastic elastomers (ETPEs) are futuristic binders for propellant/explosive formulations. Poly(glycidyl nitrate) (PGN)-based ETPEs have excellent performance, including a high energy and high oxygen content. PGN-based ETPEs were synthesized on PGN as a soft segment and hexamethylene diisocyanate extended 1,4-butanediol as a hard segment by a prepolymerization method. The thermal behavior of the PGN-based ETPEs was investigated by thermogravimetric analysis (TGA) and derivative thermogravimetry. A fitting strategy was adopted to study every stage of decomposition. The results show that the ETPEs had four main decomposition processes, and the peaks of each stage were at 212, 262, 322, and 414°C. The gas products were tested by TGA/Fourier transform infrared spectroscopy/mass spectrometry, and the main gas products of the samples were N_2O, CH_2O, C_2H_4O, and CO_2. The previous results indicate the proposed mechanism of thermal decomposition. © 2014 Wiley Periodicals, Inc. J. Appl. Polym. Sci. **2014**, *131*, 40965.

KEYWORDS: elastomers; polyurethanes; thermogravimetric analysis (TGA)

Received 1 March 2014; accepted 4 May 2014
DOI: 10.1002/app.40965

INTRODUCTION

Solid high-energy formulations comprise solid ingredients and other minor additives dispersed throughout a binder matrix. Binders provide a matrix to bind the solid ingredients together. It gives the desired shape and structural integrity to propellants or explosive charges.[1] Conventional binders use crosslinked elastomers, in which prepolymers (e.g., HTPB) are crosslinked by chemical curing/crosslinking agents. However, the disposal of the crosslinked binder is difficult and usually accomplished by burning; this causes environmental problems.[2–4] In view of the inherent disadvantages of crosslinked polymers, there has been profound interest in the development of thermoplastic elastomers (TPEs) as suitable candidates for binder applications.

Many TPEs, such as Kraton, Estane, Viton, and styrene–butadiene–styrene copolymer, have been reported in propellant/explosive compositions.[5] These polymers are nonenergetic, so they reduce the energy and overall performance of the composition. To overcome these problems, energetic thermoplastic elastomers (ETPEs) were developed. Polyoxetanes and polyoxiranes having energetic groups, such as azido, nitrato, and nitro groups, in their pendant groups have been widely reported to act as ETPEs. The ETPEs of the azido and nitrato classes have been found to be thermally stable, and their formulations are insensitive to mechanical stimuli.[6] Some of the examples of monomers with nitrato group are bis(nitrato methyl) oxetane, poly(nitrato methyl methyl oxetane), and poly(glycidyl nitrate) (PGN). PGN has been used in binders because of its high energy, high density, and high oxygen content.

PGN has been known and recognized as an energetic prepolymer since the early 1950s. The initial work on PGN was done by Thelan et al. at the Naval Ordnance Test Station (now the Naval Weapons Center). They studied the polymerization of glycidyl nitrate by a variety of Lewis acid catalysts, with most of the work centering on the use of stannic chloride as a catalyst. This was later evaluated as a propellant at the Jet Propulsion Laboratory.[7]

On the basis of the polymerization of PGN,[8–10] Diaz et al.[11] synthesized PGN-based ETPEs and studied their heats of combustion. However, there has been little study of their thermal decomposition behavior, which is very important for applications. In this study, the synthesis of PGN-based ETPEs and the features of the samples were examined. In addition, information about their thermal behavior, especially the evolution of gaseous compounds with thermogravimetric analysis (TGA)/Fourier transform infrared (FTIR) spectroscopy/mass spectrometry (MS) was obtained.

EXPERIMENTAL

Materials

PGN [number-average molecular weight (M_n) =4770 g/mol, OH equivalent = 0.454 mmol/g, Liming Research Institute of

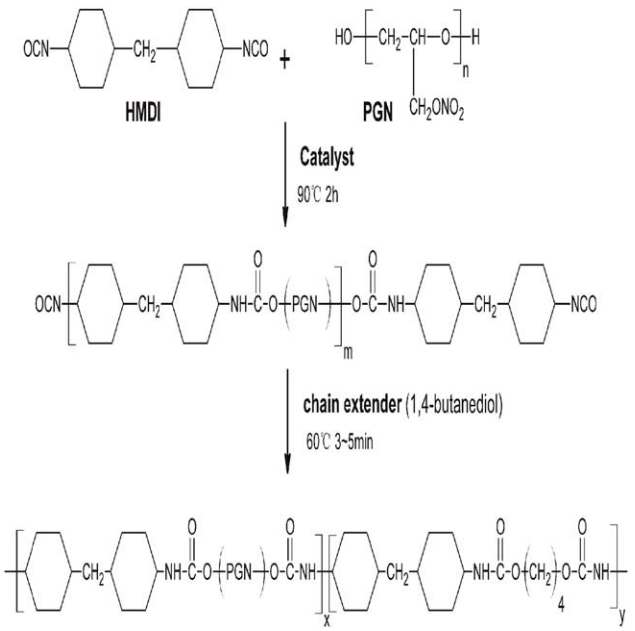

Figure 1. Synthesis process for the PGN-based ETPEs.

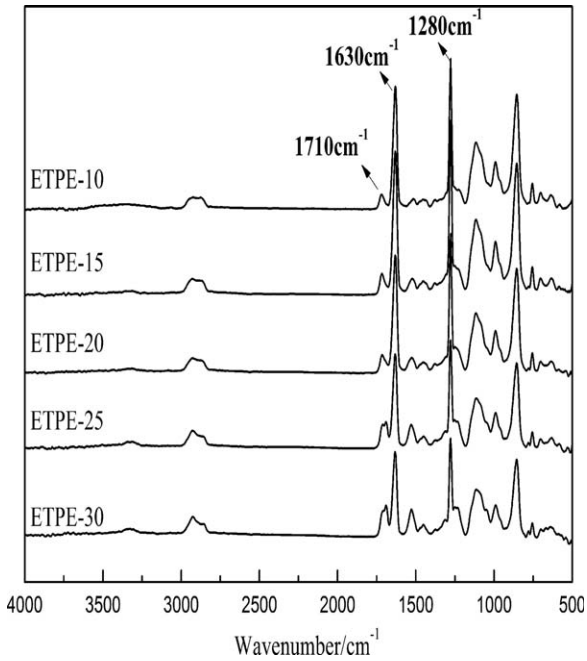

Figure 2. FTIR Spectra of the PGN-based ETPEs.

Chemical Industry, Henan China] was used after it was vacuum-dried for 2 h at 90°C. 1,4-Butanediol (BDO; $M_n = 90$ g/mol, OH equivalent = 22.22 mmol/g, Beijing Chemical Plant) was used after it was vacuum-dried for 4 h at 85°C. Hexamethylene diisocyanate (HMDI; $M_n = 250$ g/mol, Bayer Co.) was used as received. The catalyst was prepared by the dissolution of dibutyl tin dilaurate (Beijing Chemical Plant) into dibutyl phthalate.

Synthesis

A general prepolymer process was used to synthesize PGN-based ETPEs with different hard segment weight percentage ratios (10, 15, 20, 25, and 30 wt %). The hard segments consisted of HMDI chain-extended with BDO. The soft segment was PGN.

The hard-segment content (HS) by weight was determined with the industry's standard:

$$\mathrm{HS\ (wt\,\%)} = \frac{m_{\mathrm{HMDI}} + m_{\mathrm{BDO}}}{m_{\mathrm{HMDI}} + m_{\mathrm{BDO}} + m_{\mathrm{PGN}}}$$

where m_i is the mass.

The synthesis process is illustrated in Figure 1. The sample with a 10% HS was named ETPE-10, the sample with a 15% HS was named ETPE-15, and so on.

A stoichiometric amount of PGN was heated and stirred at 90°C, and then, the catalyst and HMDI were added. The reaction mixture was stirred and kept for 2 h at 90°C. BDO was added to the previous NCO-terminated PGN prepolymer at 60°C, and the reaction was kept for 3–5 min. Then, the product was cast in a mold to cure at 100°C for around 10 h. Finally, the PGN-based ETPEs with different HSs were obtained.

Measurements

IR spectra were recorded on an FTIR instrument (Nicolet FTIR-8700,Thermo) with a wave-number resolution of 4 cm^{-1} and a single average of 32 scans at room temperature. Each sample for IR analysis was obtained with attenuated total reflection.

The molecular weights [weight-average molecular weight (M_w) and M_n] and the polydispersity index (PDI = M_w/M_n) were obtained with gel permeation chromatography (GPC; LC-20A, Shimadzu). The operating temperature was 40°C, the mobile phase was tetrahydrofuran, the flow rate was 1.0 mL/min, and the raw data were calibrated with universal calibration with polystyrene standards.

TGA was carried out in a TGA analyzer (TGA/DSC1SF/417-2, Mettler Toledo) at heating rates of 10°C/min from room temperature to 600°C in a nitrogen atmosphere (40 mL/min).

The TGA/FTIR/MS experiments were performed with a thermal analyzer system coupled with an FTIR spectrometer and an MS instrument. For the TGA (TGA/DSC1SF/417-2, Mettler Toledo), we used a heating rate of 10°C/min from room temperature to 600°C in an argon atmosphere (40 mL/min). The FTIR spectroscope (Nicolet IS10, Thermo) was linked to the TGA instrument to measure the gas products. The gas lines between the TGA instrument and the FTIR instrument were heated to 220°C. The spectra were collected at a resolution of 4 cm^{-1}. The temperature of the IR cell was 230°C. The MS instrument (Omnistar/Thermostar GSD320, Pfeiffer) was linked to the FTIR spectroscope to measure the mass-to-charge ratio (m/z) of the evolved gaseous compounds. The transfer line between the FTIR spectroscope and MS instrument was maintained at 350°C. The temperature of the MS detector was 120°C.

Differential scanning calorimetry (DSC) analysis was made over the temperature range from −100 to 150°C on a Mettler DSC1 with a 10 K/min heating rate in a nitrogen atmosphere (40 mL/min). Amounts of 2–5 mg of each sample were placed in small confined aluminum cells.

Table I. Composition of PGN-Based ETPEs

	Hard segment (%)				
	10	15	20	25	30
Sample code	ETPE-10	ETPE-15	ETPE-20	ETPE-25	ETPE-30
M_n (g/mol)	31,200	29,900	30,033	30,830	31,023
M_w (g/mol)	65,520	62,192	63,669	67,826	66,078
PDI (M_w/M_n)	2.10	2.08	2.12	2.20	2.13

The stress–strain test of the elastomers was measured with a tensile testing machine (Instron-6022, Shimadzu Co., Ltd.) at a constant strain rate of 100 mm/min at room temperature.

RESULTS AND DISCUSSION

Characterization

The characterizations of the synthesized PGN-based ETPEs were performed by FTIR spectroscopy, GPC, DSC, and stress–strain test.

Figure 2 shows the IR spectra of the synthesized PGN-based ETPEs with different HS weight percentages. The IR spectra of the ETPEs did not show the absorption bands at 3350 and 2260 cm^{-1} corresponding to —OH and —NCO groups. The urethane characteristic bands at 3340 and 1710 cm^{-1} were also observed; they corresponded to the —NH stretching and C═O stretching of amide. The characteristic peaks of the —ONO_2 group from PGN at 1630 and 1280 cm^{-1} were also shown.[12,13]

The M_n, M_w, and PDI (M_w/M_n) values of the synthesized PGN-based ETPEs are shown in Table I. The M_n's of the ETPEs were around 30,000 g/mol, and the PDI values were between 2.00 and 2.20.

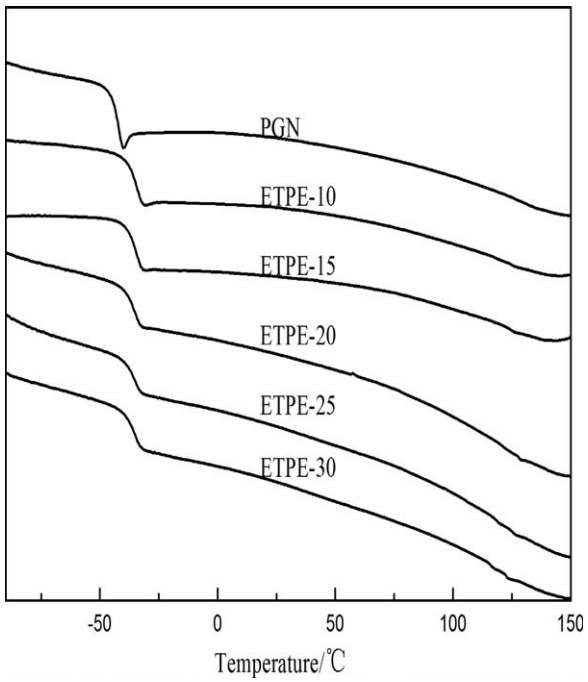

Figure 3. DSC thermograms of the PGN and PGN-based ETPEs.

Figure 3 shows the DSC thermograms of the PGN and PGN-based ETPEs with different HS weight percentages.

The glass-transition temperatures (T_g's) with different HSs are listed in Table II. As shown in Figure 3 and Table II, the T_g's of the ETPEs were all higher than that of PGN (−43.24°C). The T_g values of the PGN-based ETPEs were independent of HS; this indicated a relatively small amount of hard-segment mixing within the soft domain. Similar results were reported by Paik Sung et al.[14] for poly(tetramethylene oxide) soft-segment polyurethanes.

The stress–strain test data of the elastomers are listed in Table III, which shows the tensile results of the ETPEs. The maximum stress (σ_m) increased with HS, but the elongation at break (ε_m) decreased at higher HS values. As HS went up, stronger interactions among the polymeric chains led to stronger hydrogen bonding between hard segments and higher tensile strengths, but ε_m decreased because of these interactions.[15]

TGA/Derivative Thermogravimetry (DTG)

Thermal analysis is a frequently used tool in propellant research. Thermal decomposition can be correlated with important performance parameters, such as heat of explosion, detonation velocity, and detonation energy.[16,17] So, it was necessary to understand the thermal decomposition process of the PGN-based ETPEs.

Figure 4 shows the thermal curves of the pure hard-segment HMDI–BDO, soft-segment PGN, and ETPE-30 recorded at a heating rate of 10 K/min. In the TGA curve of PGN, two characteristic weight loss steps were observed. The first step (a) started at 170°C, ended at 250°C, and corresponded to the decomposition of —ONO_2.[18] The second stage involved the decomposition of the polyether skeleton between 250 and 430°C. These two weight loss stages were clearly depicted in the DTG curve (Figure 5). Similarly, the TGA curve of HMDI–BDO represented two major steps of mass loss, which are shown in the DTG curve of HMDI–BDO (Figure 5). The first decomposition stage (c) started at 300°C and ended at 410°C. This corresponded to the decomposition of the urethane segment. The second stage (d) corresponding to the residual hard segment was completed at nearly 520°C.

Thus, the decompositions of the soft and hard segments of ETPE overlapped. To understand the thermal decomposition

Table II. T_g Values of the PGN-Based ETPEs

Sample code	PGN	ETPE-10	ETPE-15	ETPE-20	ETPE-25	ETPE-30
T_g (°C)	−43.24	−35.38	−35.53	−35.82	−35.45	−35.87

Table III. Stress–Strain Tests for the PGN-Based ETPEs

Sample code	σ_m (MPa)	ε_m (%)
ETPE-10[a]	—	—
ETPE-15	2.176	389.363
ETPE-20	3.5230	365.500
ETPE-25	4.607	324.047
ETPE-30	4.956	312.141

[a] The ETPE-10 sample was too soft to test.

mechanism, the overlapping peaks of the DTG curve were resolved into four stages by Gaussian fitting (Figure 5). By comparing the DTG of ETPE-30 and PGN, we found that the degradation stage of ETPE-30 between 170 and 250°C corresponded to the decomposition of —ONO_2 and the stage between 220 and 300°C corresponded to the decomposition of the polyether skeleton of PGN (b).

To study the decomposition of the next two stages of the ETPEs, the DTG curves of the ETPEs with different HSs were plotted, as shown in Figure 6. As the HS increased, the third and fourth stages (c and d, respectively), due to the quantitative decomposition of hard-segment groups, became apparent. This

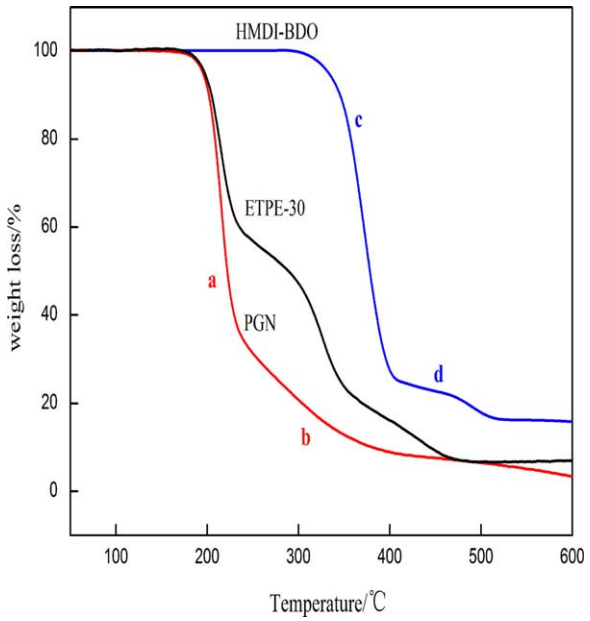

Figure 4. TGA curves of the PGN, HMDI–BDO, and ETPEs. [Color figure can be viewed in the online issue, which is available at wileyonlinelibrary.com.]

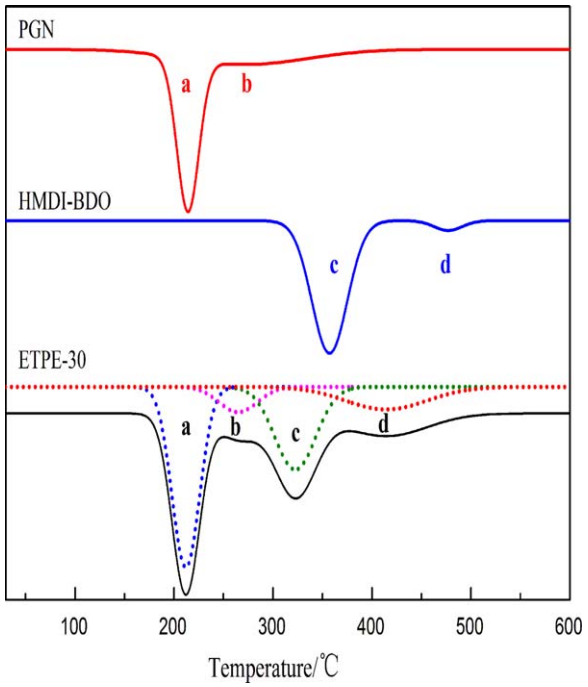

Figure 5. Derivative-of-weight-loss curves (DTG) of the PGN, HMDI–BDO, and ETPEs. [Color figure can be viewed in the online issue, which is available at wileyonlinelibrary.com.]

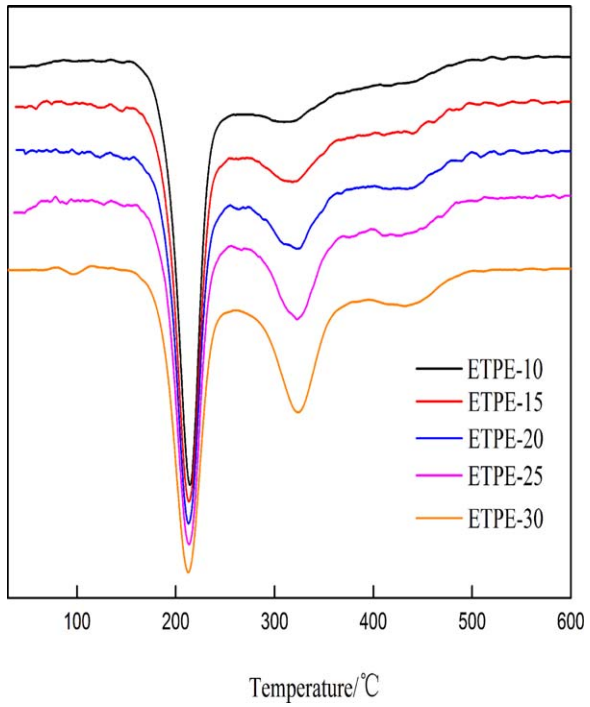

Figure 6. Derivative-of-weight-loss curves (DTG) of the ETPEs. [Color figure can be viewed in the online issue, which is available at wileyonlinelibrary.com.]

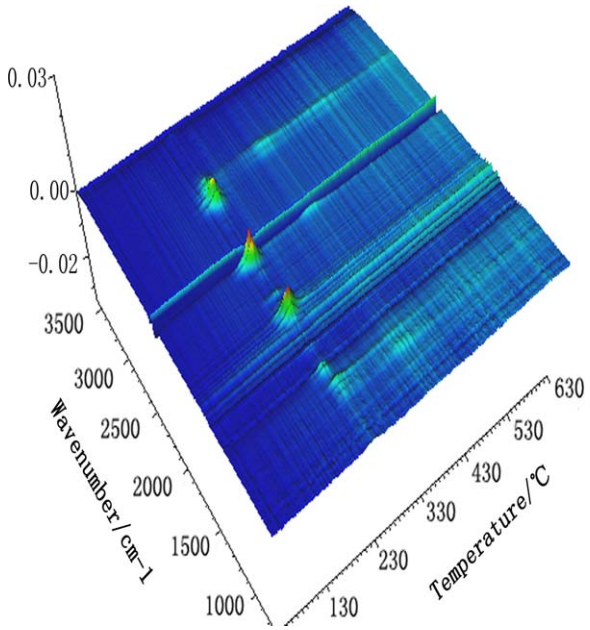

Figure 7. Three-dimensional TGA–FTIR spectra of the decomposition products of ETPE-30 during thermal degradation. [Color figure can be viewed in the online issue, which is available at wileyonlinelibrary.com.]

indicated that in the course of stages c and d were the decompositions of the hard segment. The results show that there were four stages during the ETPE thermal reactions, namely, —ONO_2 degradation, polyether skeleton degradation, urethane segment degradation, and residual hard-segment degradation. The peaks of the four stages were at 212, 262, 322, and 414°C.

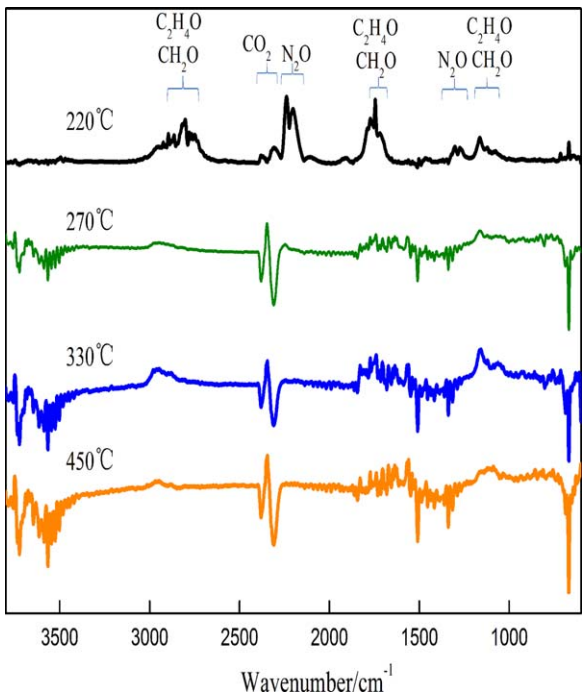

Figure 8. FTIR spectra of gas products during decomposition at respective peaks. [Color figure can be viewed in the online issue, which is available at wileyonlinelibrary.com.]

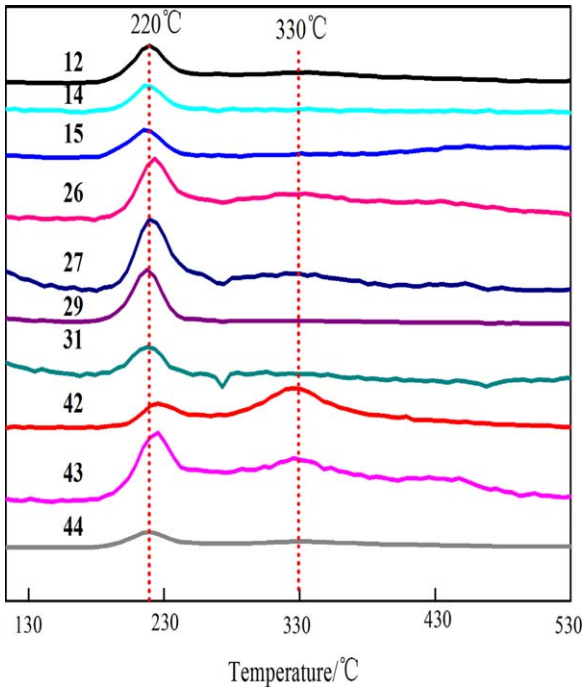

Figure 9. MS of gas products during decomposition. [Color figure can be viewed in the online issue, which is available at wileyonlinelibrary.com.]

TGA/FTIR Spectroscopy/MS

TGA has proven to be a very useful technique for studying the thermal behavior of a wide variety of solid samples. However, TGA by itself does not identify the decomposition products. When TGA is coupled with evolved gas analysis, a great deal of additional information can be obtained.

The three-dimensional TGA–FTIR spectra of the decomposition products of ETPE-30 during the thermal degradation are shown in Figure 7. The peaks shifted to a higher temperature than that of the corresponding DTG curve because of the delay time between the gas generation and its detection by the FTIR equipment. The FTIR spectra of the gas products during decomposition at their respective peaks are presented in Figure 8. The primary evolved products mainly came from the two degradation stages of the PGN segment and urethane segment (170–250 and 280–380°C). The gas products at 220°C were identified as CH_2O, C_2H_4O, or their mixture (1000–1200, 1718–1772, and 2750–3000 cm^{-1}, respectively) and N_2O (1274–302 and 2202–2238 cm^{-1}). In addition, CO_2 (2360 and 666 cm^{-1}) was emitted in this degradation stage. In the pyrolysis process at 330°C, the emission of CH_2O, C_2H_4O, or their mixture was obvious by the appearance of absorption bands at 1000–1200 and 2750–3000 cm^{-1}.

To investigate further, we studied the MS of the gas products. Figure 9 presents the evolution curves of CO_2 ($m/z = 12$ and 44), N_2O ($m/z = 14$, 15, and 31), CH_2O ($m/z = 29$), and C_2H_4O ($m/z = 26$, 27, 29, 42, and 43) during pyrolysis of the ETPEs.[19] Just like in the FTIR analysis of the gas products, the ion fragments from the products occurred mainly in two stages: 170–250and 280–380°C. At 220°C, the evolutions of N_2O, CO_2, CH_2O, and C_2H_4O occurred; these corresponded to the

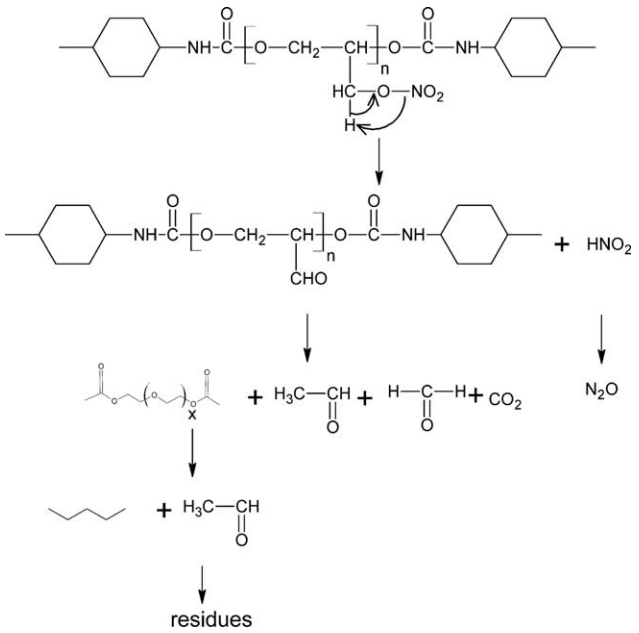

Figure 10. Decomposition mechanism of the PGN-based ETPEs.

decomposition of the PGN segment. At 330°C, C_2H_4O, which corresponded to the degradation of the urethane segment, was observed, and this was different from pure PGN.

The data of TGA/FTIR spectroscopy/MS showed that the main gas products of ETPE were N_2O, CO_2, CH_2O, and C_2H_4O. On the basis of the related references and the results of the study, the mechanism of thermal decomposition was speculated.[18] Initially, the decomposition, —ONO_2 was hydrogenated to produce HNO_2, and then, HNO_2 further decomposed to N_2O. At the same time, —CHO initiated the decomposition of the backbone. The speculative decomposition mechanism is shown in Figure 10.

CONCLUSIONS

PGN-based ETPEs were synthesized on PGN as a soft segment and HMDI extended BDO as a hard segment. From the GPC and FTIR results, the ETPEs were also synthesized successfully via a prepolymer process. In addition, the T_g values of the ETPEs were all higher than those of PGN and independent of HS. The stress–strain tests showed that ε_m decreased and σ_m increased with increasing HS.

The TGA/DTG results show that there were four stages during the ETPE thermal reactions, namely, —ONO_2 degradation, polyether skeleton degradation, urethane segment degradation, and residual hard-segment degradation. The peaks of each stage were at 212, 262, 322, and 414°C.

The thermal behavior and thermal degradation mechanism of ETPE were studied by means of the TGA/FTIR/MS coupled method; the primary evolved products mainly came from the two degradation stages of PGN (at 170–250 and 280–380°C). The main gas products of the stage at 170–250°C were N_2O, CO_2, CH_2O, and C_2H_4O; this corresponded to the decomposition of —ONO_2. The gas products of the stage at 280–380°C were C_2H_4O; this came from the degradation of the urethane segment.

ACKNOWLEDGMENTS

The project was supported by the State Key Laboratory of Explosion Science and Technology (contract grant number YBKT15-02).

REFERENCES

1. Zukas, J. A.; Walters, W. Explosive Effects and Applications; Springer: New York, **1998**.
2. Wardle, R. B. U.S. *Pat.* 4,806,613 (**1989**).
3. Miller, R. S. *Res. Soc. Symp. Proc.* **1996**, *418*, 3.
4. Murphy, E. A.; Ntozakhe, T.; Murphy, C. J.; Fay, J. J.; Sperling, L. H. *J. Appl. Polym. Sci.* **1989**, *37*, 267.
5. Sanghavi, R. R.; Asthana, S. N.; Karir, J. S. *J. Energy Mater.* **2001**, *19*, 79.
6. Sikder, A. K.; Reddy, S. *Propellants Explos. Pyrotech.* **2013**, *38*, 14.
7. Day, R. S.; Stern, A. G.; Willer, R. L. U.S. *Pat.* 5,120,827 (**1992**).
8. Braithwaite, P. C.; Lund, G. K.; Wardle, R. B. U.S. *Pat.* 5,587,553 (**1994**).
9. Sanderson, A. J.; Martins, L. J.; Dewey, M. A. U.S. *Pat.* 6,861,501B1 (**2002**).
10. Sanderson, A. J.; Martins, L. J. U.S. *Pat. 6,730*,181 B1 (**2002**).
11. Diaz, E.; Brousseau, P.; Ampleman, G.; Prud'homme, R. E. *Propellants Explos. Pyrotech.* **2003**, *28*, 101.
12. You, J. S.; Kweon, J. O.; Kang, S. C.; Noh, S. T. *Macromol. Res.* **2010**, *18*, 1226.
13. Fei, P. L.; Lin, Y.; Gang, Y. L.; De, F. N. *Polym. Bull.* **2011**, *66*, 503.
14. Paik Sung, C. S.; Hu, C. B.; Wu, C. S. *Macromolecules* **1980**, *13*, 111.
15. Yang, J. H.; Chun, B. C.; Chung, Y. C.; Cho, G. H. *Polymer* **2003**, *44*, 3251.
16. Herder, G.; Weterings, F. P.; de Klerk, W. P. C. *J. Therm. Anal. Calorim.* **2003**, *72*, 921.
17. Krabbendam-La Haye, E. L.; de Klerk, W. P.; Miszczak, M.; Szymanowski, J. *J. Therm. Anal. Calorim.* **2003**, *72*, 931.
18. Hai, C. *Initiators Pyrotech.* **2007**, *2*, 32.
19. Wei, L. C.; Xian, C. Y.; Geng, X. T. *Chem. World* **2000**, *4*, 181.